Matthews, *Proc. Natl. Acad. Sci. U.S.A.* **88**, 3441 (1991).
19. I. K. McDonald and J. M. Thornton, *J. Mol. Biol.* **238**, 777 (1994).
20. E. N. Baker and R. E. Hubbard, *Prog. Biophys. Mol. Biol.* **44**, 97 (1984).
21. A. Baird, D. Schubert, N. Ling, R. Guillemin, *Proc. Natl. Acad. Sci. U.S.A.* **85**, 2324 (1988).
22. W. F. Heath, A. S. Cantrell, N. G. Mayne, S. R. Jaskunas, *Biochemistry* **30**, 5608 (1991).
23. S. Guimond, M. Maccarana, B. B. Olwin, U. Lindahl, A. C. Rapraeger, *J. Biol. Chem.* **268**, 23906 (1993).
24. M. Maccarana, B. Casu, U. Lindahl, *ibid.*, p. 23898.
25. H. Habuchi *et al.*, *Biochem. J.* **285**, 805 (1992).
26. D. Aviezer *et al.*, *J. Biol. Chem.* **269**, 114 (1994).
27. A. T. Chellaiah, D. G. McEwen, S. Werner, J. Xu, D. M. Ornitz, *ibid.*, p. 11620.
28. C. G. Glabe, P. K. Harty, S. D. Rosen, *Anal. Biochem.* **130**, 287 (1983).
29. A. McPherson, *Eur. J. Biochem.* **189**, 1 (1990).
30. M. G. Rossmann, in *International Scientific Review Series* (Gordon and Breach, New York, 1972), vol. 13.
31. A. T. Brünger, *Acta Crystallogr.* **46**, 46 (1990).
32. W. I. Weis, A. T. Brünger, J. J. Skehel, D. C. Wiley, *J. Mol. Biol.* **212**, 737 (1990).
33. T. A. Jones and S. Thirup, *EMBO J.* **5**, 819 (1986).
34. T. A. Jones, J. Y. Zou, S. W. Cowan, M. Kjeldgaard, *Acta Crystallogr.* **47**, 110 (1991).
35. A. Roussel and C. Cambillau, TURBO-FRODO, in *Silicon Graphics Geometry Partners Directory* (Silicon Graphics, Summit, NJ, 1991), p. 86.
36. A. T. Brünger, *X-PLOR Manual, Version 3.1* (Yale University, New Haven, CT, 1992).
37. L. W. Burrus and B. B. Olwin, *J. Biol. Chem.* **264**, 18647 (1989).
38. P. J. Kraulis, *J. Appl. Crystallogr.* **24**, 946 (1991).
39. C. Svahn, A. Ansari, T. Wehler, unpublished data.
40. H. Mach *et al.*, *Biochemistry* **32**, 5480 (1993).
41. We thank D. McEwen and S. Mathews for discussion and A. Chellaiah, T. Opera, J. Xu, and M. Weurffel for help. The bFGF and antibody DG2 were gifts from J. Abraham (Scios Nova) and W. Herblin (DuPont-Merck), respectively. The aFGF and the aFGF antiserum were a gift from K. Thomas (Merck). Fluoresceinated heparin was a gift from C. Parish (Australian National University, Canberra, Australia). SOS was from Bukh Meditec. Heparin was from Hepar Inc. Supported in part by grants from NIH (CA60673), Monsanto-Searle, the Beckman Young Investigators Program (D.M.D.), and Washington University Medical School.

4 October 1994; accepted 5 January 1995

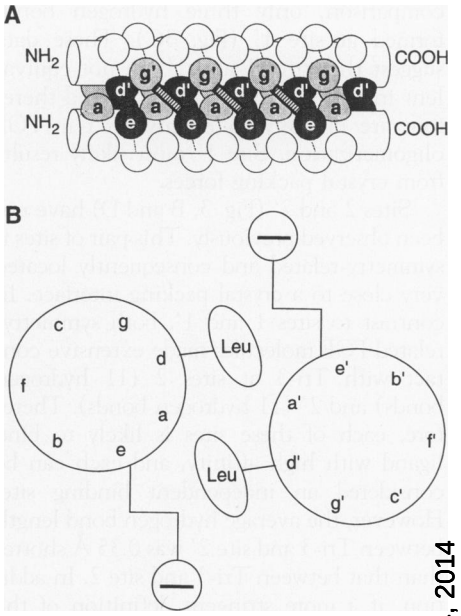

Fig. 1. (**A**) Schematic representation of the leucine zipper, a parallel, two-stranded coiled coil (*4*). A side view is shown. For simplicity, the supercoiling of the helices is not depicted. The sequences of coiled coils are characterized by a heptad repeat of seven amino acid residues, denoted **a** to **g** (*7*). Prime (′) refers to positions from the other helix. Most of the residues at positions **a** and **d** are hydrophobic, forming the characteristic 4-3 repeat of coiled coils, whereas residues at positions **e** and **g** are often charged (*7*, *26*). The hydrophobic interface between the two α helices is formed by residues at positions **a**, **d**, **e**, and **g** (*4*). One set of packing interactions consists of side chains from positions **a**, **a′**, **g** and **g′** (light shading), whereas the second set consists of side chains from positions **d**, **d′**, **e**, and **e′** (dark shading). Residues at positions **g′** and **e** pack against positions **a** and **d′**, respectively, and can participate in interhelical electrostatic interactions from position **e** to **g′** of the preceding heptad (indicated with ladders). (**B**) Schematic cross section through the dimer, depicting packing interactions between the residues at positions **d** and **e** (*4*). As an example, leucine at position **d** and glutamic acid at position **e** is shown. The large circles represent the helical backbone and the line segments represent bonds between carbon atoms. Residues at **d** and **d′** make side-to-side interactions. Additionally, methylene groups from residues at positions **e** and **e′** make contacts with the hydrophobic residues at positions **d** and **d′**. These types of interactions are also present in the **a** layer, in which residues from positions **g** and **g′** make contacts with residues at positions **a** and **a′**.

Measurement of Interhelical Electrostatic Interactions in the GCN4 Leucine Zipper

Kevin J. Lumb and Peter S. Kim*

The dimerization specificity of the bZIP transcription factors resides in the leucine zipper region. It is commonly assumed that electrostatic interactions between oppositely charged amino acid residues on different helices of the leucine zipper contribute favorably to dimerization specificity. Crystal structures of the GCN4 leucine zipper contain interhelical salt bridges between Glu^{20} and $Lys^{15'}$ and between Glu^{22} and $Lys^{27'}$. ^{13}C–nuclear magnetic resonance measurements of the glutamic acid pK_a values at physiological ionic strength indicate that the salt bridge involving Glu^{22} does not contribute to stability and that the salt bridge involving Glu^{20} is unfavorable, relative to the corresponding situation with a neutral (protonated) Glu residue. Moreover, the substitution of Glu^{20} by glutamine is stabilizing. Thus, salt bridges will not necessarily contribute favorably to bZIP dimerization specificity and may indeed be unfavorable, relative to alternative neutral-charge interactions.

Transcription factors of the basic-region leucine zipper (bZIP) family bind to DNA as homo- or heterodimers (*1*). Dimerization of these proteins is controlled by the leucine zipper (Fig. 1A), a parallel, two-stranded coiled coil (*2*–*4*). The leucine zipper thus mediates the DNA-binding specificity of the bZIP transcription factors by determining which bZIP proteins form stable dimers. Accurate prediction of bZIP dimerization specificity will require an understanding of the principles governing leucine zipper dimerization.

The formation of favorable hydrophobic packing interactions involving residues at positions **a** and **d** of the coiled-coil heptad repeat, and including the side chains of residues at positions **e** and **g** (Fig. 1B), can contribute to dimerization specificity. Residues at the **e** and **g** positions also can contribute substantially to the specificity of leucine zipper dimerization through interhelical electrostatic interactions (Fig. 1A). Previous studies have demonstrated that the dimerization specificity of both the Fos-Jun oncoprotein (*5*) and a de novo designed heterodimeric coiled coil (*6*) results largely from the relief of unfavorable interhelical electrostatic interactions between residues of like charge in the homodimers. Thus, avoidance of electrostatic repulsion is an important determinant of dimerization specificity (*5*, *6*).

Conversely, it is often assumed that formation of favorable electrostatic interactions between the helices contributes to the global stability and dimerization specificity of two-stranded coiled coils (*4*, *7*–*12*). Indeed, crystal structures of leucine zippers (*4*, *10*, *11*) show interhelical salt bridges between charged residues at **g′** positions to residues of opposite charge, on the other helix, at **e** positions of the following heptad (Fig. 1A).

GCN4-p1 is a synthetic peptide corresponding to the leucine zipper of the yeast transcriptional activator GCN4 (Fig. 2A). Interhelical salt bridges are observed in the crystal structure of GCN4-p1 (*13*) between

Howard Hughes Medical Institute, Whitehead Institute for Biomedical Research, Department of Biology, Massachusetts Institute of Technology, Nine Cambridge Center, Cambridge, MA 02142, USA.

*To whom correspondence should be addressed.

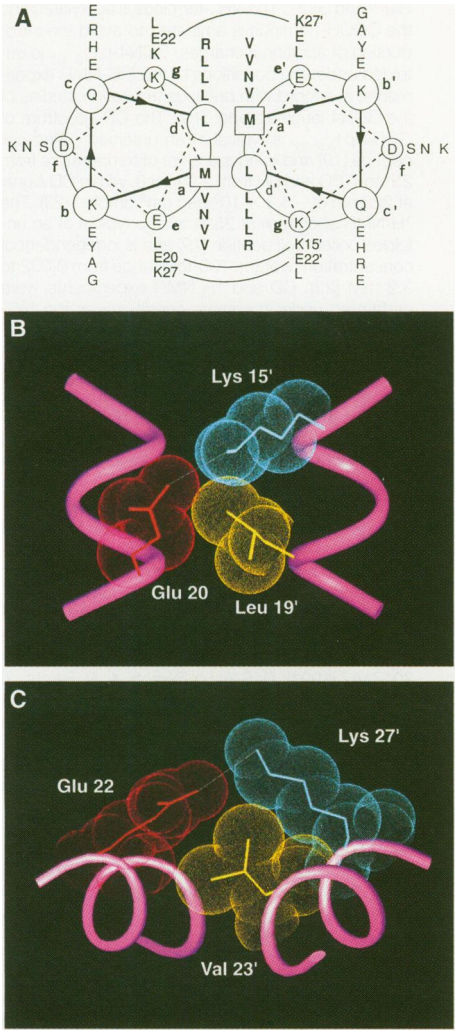

Fig. 2. (**A**) Helical wheel representation of residues 2 to 31 of GCN4-p1 (*3*). Residues that form interhelical salt bridges in the crystal structure of GCN4-p1 are connected by curved lines (*13*). The $Glu^{20'}$-Lys^{15} salt bridge is not present in the crystal structure of GCN4-p1 (*13*). The peptide corresponds to the COOH-terminal 33–amino acid leucine-zipper region (residues 249 to 281) of GCN4. The NH_2-terminus is acetylated. The COOH-terminus is free, as in GCN4. The helical wheel view is from the NH_2-terminus. (**B**) The Glu^{20}-$Lys^{15'}$ salt bridge of the GCN4-p1 crystal structure (*13*). Also shown is the $Leu^{19'} \rightarrow Glu^{20}$ (**d'** → **e**) packing interaction (see also Fig. 1B). (**C**) The Glu^{22}-$Lys^{27'}$ salt bridge of the GCN4-p1 crystal structure (*13*). Also shown is the $Glu^{22} \rightarrow Val^{23'}$ (**g** → **a'**) packing interaction (see also Fig. 1B).

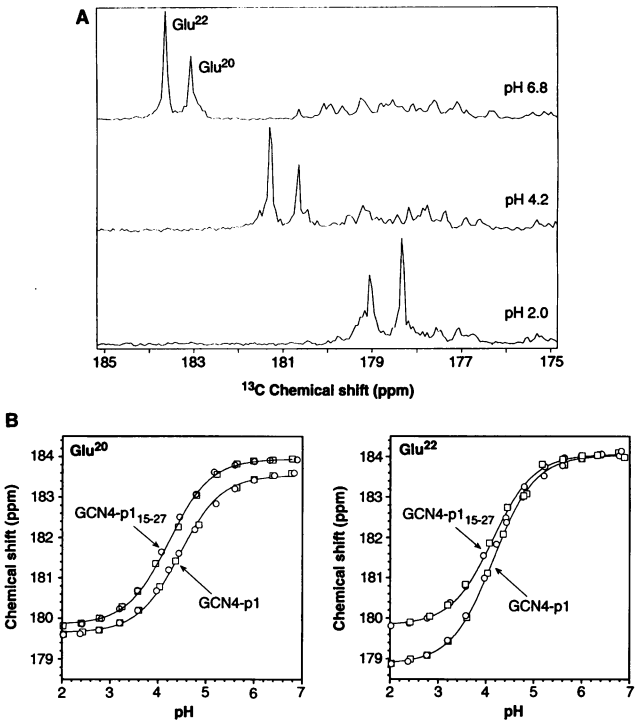

Fig. 3. (**A**) ^{13}C-NMR spectra of GCN4-p1 (*24*). Approximately 10% and 20% of Glu^{20} and Glu^{22}, respectively, have been enriched with ^{13}C at the carboxylate carbon (*16*). Thus, the carboxylate carbon resonance of Glu^{22} has twice the intensity of that from Glu^{20}, allowing the resonances to be assigned unambiguously. (**B**) The pK_a values of Glu^{20} and Glu^{22} in GCN4-p1 and the unfolded-control peptide GCN4-$p1_{15-27}$ were measured at 25°C and physiological ionic strength (10 mM sodium phosphate, 150 mM NaCl) from the changes in the ^{13}C chemical shift of the carboxylate carbons with pH. Two independent sets of data are shown as circles and squares. The curves are least-squares fits to the Henderson-Hasselbach equation (*27*).

Glu^{20} and $Lys^{15'}$ (Fig. 2B) and between Glu^{22} and $Lys^{27'}$ (Fig. 2C). These salt bridges are also present in crystal structures of the GCN4 bZIP domain bound to DNA (*13*).

The effect on stability of titrating a charged residue ($\Delta\Delta G_{titr}$) can be determined directly from the difference in the pK_a values (where pK_a is the acid constant) in the folded and unfolded states (*14*). An acidic residue involved in a stabilizing salt bridge will have a lower pK_a in the folded than in the unfolded state. For example, the pK_a of Asp^{70}, which forms a partially buried salt bridge with His^{31} in T4 lysozyme, is lowered by at least 3.5 units relative to the unfolded state (*15*). Conversely, if the net electrostatic interaction between an acidic residue and the rest of the environment is unfavorable (destabilizing) in the folded relative to the unfolded state, the pK_a will be increased relative to the unfolded-state value.

We measured by ^{13}C–nuclear magnetic resonance (NMR) the pK_a values of Glu^{20} and Glu^{22} in GCN4-p1. Glutamic acid enriched with ^{13}C at the carboxylate δ-carbon was incorporated by peptide synthesis at residues 20 and 22 of GCN4-p1 at levels of approximately 10 and 20%, respectively (*16*). This allowed unambiguous assignment of the Glu^{20} and Glu^{22} carboxylate ^{13}C-resonances (Fig. 3A). We measured the pK_a values at physiological ionic strength by following the change in chemical shift of the carboxylate resonance with pH (Fig. 3).

The unfolded-state pK_a values were measured in the same way in GCN4-$p1_{15-27}$, a peptide model of the unfolded state of GCN4-p1 that corresponds to residues 15 to 27. Circular dichroism (CD) and ^1H-NMR studies indicate that GCN4-$p1_{15-27}$ is unfolded (*17*). This unfolded-state model permits pK_a shifts to be measured without the need to make corrections for the effects of chemical denaturants or temperature or to assume a generic, unperturbed pK_a value in the unfolded state (*18*).

If the interhelical salt bridges in GCN4-p1 are stabilizing relative to the corresponding situation with a charged Lys and a neutral (protonated) Glu residue, the pK_a values of Glu^{20} and Glu^{22} would be lower in the folded than in the unfolded state. Instead, at physiological ionic strength, the pK_a of Glu^{22} is unperturbed (the folded- and unfolded-state pK_a values are 4.13 ± 0.05 and 4.12 ± 0.05, respectively; Fig. 3B). The pK_a of Glu^{20} is actually shifted higher in the folded state (Fig. 3B), indicating that the ionized Glu^{20} residue is destabilizing by 0.3 ± 0.1 kcal/mol (given by $\Delta\Delta G_{titr} = -2.303RT\Delta pK_a$; the folded- and unfolded-state pK_a values are 4.44 ± 0.05 and 4.20 ± 0.05, respectively).

We conclude that the salt bridges observed in the crystal structures of GCN4-p1 and the GCN4 bZIP-DNA complexes either do not form in solution or that the contribution of these salt bridges to stability is negligible at best, relative to when only the Lys residue is charged. This conclusion is in accord with the very slight dependence of the thermal stability of GCN4-p1 on pH or ionic strength (*6*, *19*) and earlier studies indicating that surface salt bridges, in general, contribute only marginally (~0.5 kcal/mol or less) to protein stability (*14*, *20*).

It is particularly surprising that the pK_a of Glu^{20} is slightly increased in the folded state, indicating that the charged form of this residue is slightly destabilizing relative to the neutral form. This conclusion is corroborated by the increased thermal stability at pH 7 of the variant of GCN4-p1 with the substitution $Glu^{20} \rightarrow Gln$ (*21*). It is unclear why a negative charge at position 20 is destabilizing, although one possible explanation is that the neutral form of Glu^{20} (or

a Gln residue) packs more favorably than the ionized form of Glu^{20} against residues in the dimer interface (Figs. 1B and 2B). It may also be noteworthy that the Glu^{20}-$Lys^{15'}$ salt bridge packs against $Asn^{16'}$, in a region of potential asymmetry (*13*).

Residues at positions **e** and **g** contribute to coiled-coil dimerization specificity both by forming favorable packing interactions at the hydrophobic interface (Fig. 1B) and by destabilizing dimers via unfavorable interhelical electrostatic interactions (*5*, *6*). It is often assumed that favorable electrostatic interactions, resulting from interhelical salt bridges, are also critical determinants of dimerization specificity (*4*, *7*–*12*). Our results challenge this assumption and indicate instead that the formation of salt-bridge interactions should not be weighed more heavily than the formation of alternative neutral-charge interactions in the prediction of bZIP and coiled-coil dimerization specificity.

Note added in proof: Recent double-mutant cycle studies of a putative salt bridge in a designed coiled coil suggest that a neutral Glu-charged Lys interaction is 0.2 kcal/mol more stable than a charged Glu-charged Lys interaction. No structural evidence exists, however, for salt bridges in this coiled coil (*22*).

REFERENCES AND NOTES

1. For a recent review, see T. Ellenberger, *Curr. Opin. Struct. Biol.* **4**, 12 (1994).
2. W. H. Landschulz, P. F. Johnson, S. L. McKnight, *Science* **240**, 1759 (1988).
3. E. K. O'Shea, R. Rutkowski, P. S. Kim, *ibid.* **243**, 538 (1989). The sequence of GCN4-p1 is acetyl-RMKQLEDKVEELLSKNYHLENEVARLKKLVGER. Abbreviations for the amino acid residues are as follows: A, Ala; D, Asp; E, Glu; G, Gly; H, His; K, Lys; L, Leu; M, Met; N, Asn; Q, Gln; R, Arg; S, Ser; V, Val; and Y, Tyr.
4. E. K. O'Shea, J. D. Klemm, P. S. Kim, T. Alber, *Science* **254**, 539 (1991). The 1.8 Å crystal structure of GCN4-p1 was determined from crystals obtained at pH 7.2 from 25 mM sodium phosphate, 0.4 M NaCl with polyethylene glycol as the precipitant.
5. E. K. O'Shea *et al.*, *Science* **245**, 646 (1989); E. K. O'Shea *et al.*, *Cell* **66**, 699 (1992); M. John *et al.*, *J. Biol. Chem.* **269**, 16247 (1994).
6. Electrostatic destabilization of homodimers has been used as a protein design principle to make two peptides with "Velcro"-like properties [E. K. O'Shea, K. J. Lumb, P. S. Kim, *Curr. Biol.* **3**, 658 (1993)] that have been used to bring together two proteins in vivo [H. Chang *et al.*, *Proc. Natl. Acad. Sci. U.S.A.* **91**, 11408 (1994)]. The two peptides form a stable heterodimeric coiled coil, but the individual peptides do not form stable homodimers. The heterodimer has a dissociation constant of 30 nM, and there is at least a 10^5-fold preference for heterodimer formation, at pH 7 and 20°C in phosphate-buffered saline (10 mM sodium phosphate, 150 mM NaCl). The pH and ionic strength dependence of stability, and pK_a measurements indicate that the heterodimerization specificity results predominantly from electrostatic destabilization of the homodimers [related strategies have also been described (*9*)]. The heterodimer has amide protons that are protected from hydrogen exchange by factors that would be expected if exchange only occurred from globally unfolded molecules; this property strongly suggests that the designed peptide has a well-defined structure, in contrast to other designed peptides and proteins [S. F. Betz, D. P. Raleigh, W. F. DeGrado, *Curr. Opin. Struct. Biol.* **3**, 601 (1993)].
7. A. D. McLachlan and M. Stewart, *J. Mol. Biol.* **98**, 293 (1975).
8. D. Stone, J. Sodek, P. Johnson, L. B. Smillie, in *Proteins of Contractile Systems*, E. N. A. Biro, Ed. (North-Holland, Amsterdam, 1975), pp. 125–136; J. A. Talbot and R. S. Hodges, *Acc. Chem. Res.* **15**, 224 (1982); K. T. O'Neil and W. F. DeGrado, *Science* **250**, 646 (1990); M. Nilges and A. T. Brünger, *Protein Eng.* **4**, 649 (1991); M. Schuermann, J. B. Hunter, G. Hennig, R. Müller, *Nucleic Acids Res.* **19**, 739 (1991); M. Engel, R. W. Williams, B. W. Erickson, *Biochemistry* **30**, 3161 (1991); K. S. Thompson, C. R. Vinson, E. Freire, *ibid.* **32**, 5491 (1993); B. Amati *et al.*, *Cell* **72**, 233 (1993); C. Cohen and D. A. D. Parry, *Science* **263**, 488 (1994); A. Letai and E. Fuchs, *Proc. Natl. Acad. Sci. U.S.A.* **92**, 92 (1995).
9. T. J. Graddis *et al.*, *Biochemistry* **32**, 12664 (1993); N. E. Zhou *et al.*, *J. Mol. Biol.* **237**, 500 (1994).
10. T. E. Ellenberger *et al.*, *Cell* **71**, 1223 (1992).
11. P. Konig and T. J. Richmond, *J. Mol. Biol.* **233**, 139 (1993).
12. D. Krylov *et al.*, *EMBO J.* **13**, 2849 (1994).
13. The crystal structures of GCN4-p1 (*4*) and of GCN4 bZIP domains bound to the AP-1 (*10*) and ATF-CREB (*11*) DNA sites contain interhelical salt bridges between Glu^{22} and $Lys^{27'}$, and between $Glu^{22'}$ and Lys^{27} ($Glu^{270'}$ and Lys^{275}, respectively, in GCN4). The GCN4-p1 (*4*) and AP-1 cocrystal (*10*) structures contain interhelical salt bridges between Glu^{20} and $Lys^{15'}$ (Glu^{268} and $Lys^{263'}$, respectively, in GCN4). The reciprocal $Glu^{20'}$-Lys^{15} salt bridge is not seen in the crystal structure of GCN4-p1 owing to a region of asymmetry around Asn^{16} [figure 6D of (*4*)] and is blocked in the AP-1 structure by symmetry-related DNA in the crystals (*10*). Interhelical salt bridges involving Glu^{20} and Lys^{15} are not observed (ion-pair distance = 6.0 Å) on either side of the dimer in the ATF-CREB cocrystal structure, which has crystallographically imposed symmetry in the region of Asn^{16} (*11*). If the asymmetry observed in the GCN4-p1 (*4*) and bZIP-AP-1 (*10*) crystal structures also existed in solution, then the different environment of each monomer would usually result in two resonances for each nucleus. Only one resonance is observed for the γ-^{13}C (Fig. 3A) and ^1H nuclei of GCN4-p1 [T. G. Oas, L. P. McIntosh, E. K. O'Shea, F. W. Dahlquist, P. S. Kim, *Biochemistry* **29**, 2891 (1990)], indicating either that GCN4-p1 is symmetrical in solution or that the different asymmetric conformations are in fast exchange on the chemical-shift time scale. Amide proton exchange rates in a GCN4 leucine zipper peptide are faster on average for the heptad sequence containing Asn^{16} than for the other heptad repeats, suggesting that the region near Asn^{16} has greater motional flexibility than other regions of the leucine zipper [E. M. Goodman and P. S. Kim, *Biochemistry* **30**, 11615 (1991)].
14. J. G. Kirkwood and F. H. Westheimer, *J. Chem. Phys.* **6**, 506 (1938); A. Yang and B. Honig, *Curr. Opin. Struct. Biol.* **2**, 40 (1992).
15. D. E. Anderson, W. J. Becktel, F. W. Dahlquist, *Biochemistry* **29**, 2403 (1990).
16. Peptides were synthesized with solid-phase *t*-Boc methods as described (*3*). (δ-^{13}C, 99%) *t*-Boc-Glu-(OBzl) was obtained from Cambridge Isotope Laboratories, Andover, MA. Glu^{20} and Glu^{22} were coupled in two steps. ^{13}C-labeled Glu was first coupled at less than stoichiometric amounts, with ~10 and 20% coupling of ^{13}C-labeled Glu at residues 20 and 22, respectively. The extent of coupling was determined with the ninhydrin reaction [V. K. Sarin, S. B. H. Kent, J. P. Tam, R. B. Merrifield, *Anal. Biochem.* **117**, 147 (1981)]. Coupling was taken to completion in the second step with unlabeled Glu. Final purification was by reversed-phase high-performance liquid chromatography on a Vydac C_{18} column with a linear water-acetonitrile gradient containing 0.1% trifluoroacetic acid. The identity of each peptide was confirmed by laser desorption mass spectrometry on a Finnigan Lasermat. For each peptide, the expected and observed molecular masses agreed to within 1 dalton.
17. GCN4-$p1_{15-27}$ corresponds to residues 15 to 27 of GCN4-p1 and contains five residues before and after Glu^{20} and Glu^{22}. The NH_2-terminus is acetylated and the COOH-terminus is amidated to avoid the introduction of additional charges. GCN4-$p1_{15-27}$ is unfolded under the conditions of the ^{13}C-NMR experiments, in accord with previous truncation studies of the GCN4 leucine zipper (*19*). The CD spectrum of GCN4-$p1_{15-27}$ is typical of an unfolded coiled-coil peptide (*19*) and is independent of temperature from 25° to 70°C and pH from 2.0 to 6.8, with a CD signal at 222 nm of -5.3×10^3 deg cm^2 dmol^{-1} (*23*). The ^1H-NMR spectrum at 25°C is also typical of an unfolded coiled-coil peptide (*19*) and is independent of concentration over the 100-fold range from 0.032 to 3.2 mM (*23*). CD and ^1H-NMR experiments were performed under the same conditions as the ^{13}C-NMR experiments (*24*).
18. The pK_a of AcGluOMe is 4.3 ± 0.1 (*23*, *24*), which is slightly higher than that found for Glu^{20} and Glu^{22} in the unfolded-model peptide GCN4-$p1_{15-27}$ (Fig. 3B). This illustrates the importance of making measurements in a good peptide model for the unfolded state, rather than relying on the intrinsic pK_a of an isolated, blocked amino acid.
19. K. J. Lumb *et al.*, *Biochemistry* **33**, 7361 (1994).
20. The marginal contribution of surface salt bridges to stability is attributed to the high dielectric of the solvent, which reduces the strength of a surface ionic interaction, and to the unfavorable energetic penalties of desolvating the charges and locating the mobile charged groups in a salt bridge [S. Dao-pin, U. Sauer, H. Nicholson, B. W. Matthews, *Biochemistry* **30**, 7142 (1991); D. Sali, M. Bycroft, A. R. Fersht, *J. Mol. Biol.* **220**, 779 (1991); Z. S. Hendsch and B. Tidor, *Protein Sci.* **3**, 211 (1994)]. The interaction energy between two opposite charges can, however, be substantial if the side chains are constrained by other features of the protein structure (*14*), and large pK_a shifts have been observed in proteins [(*15*); A. R. Fersht, *Cold Spring Harbor Symp. Quant. Biol.* **36**, 71 (1972)]. It is possible, therefore, that salt bridges in other coiled coils are more stabilizing than in the GCN4 leucine zipper [see also (*12*). In particular, the salt bridges observed in three- and four-stranded GCN4 leucine zipper variants [P. B. Harbury, T. Zhang, P. S. Kim, T. Alber, *Science* **262**, 1401 (1993); P. B. Harbury, P. S. Kim, T. Alber, *Nature* **371**, 80 (1994)] are shorter and less solvent exposed than those seen in the GCN4-p1 crystal structure.
21. The midpoints of thermal denaturation (T_m) at pH 7.0 of GCN4-p1 and the $Glu^{20} \rightarrow$ Gln variant are 56° and 58°C, respectively. At pH 2, however, GCN4-p1 is more stable than the Gln variant (the T_m values are 50° and 47°C, respectively), indicating that Gln is not intrinsically stabilizing. These results strongly suggest that the neutral (protonated) form of Glu is stabilizing relative to the ionized form, in accord with the pK_a measurements. The T_m values were determined for 35 μM (monomer) samples (*25*) in 10 mM sodium phosphate, 150 mM NaCl (pH 7.0) as described (*19*). All thermal melts were reversible (the folding and unfolding curves were superimposable, with over 90% of the starting signal regained on cooling).
22. N. E. Zhou, C. M. Kay, R. S. Hodges, *Protein Sci.* **7**, 1365 (1994).
23. K. J. Lumb and P. S. Kim, unpublished data.
24. ^{13}C-NMR spectroscopy was performed on a Bruker AMX 500 spectrometer at 125.8 MHz. One-dimensional data sets defined by 4096 complex points were acquired with a spectral width of 26315.8 Hz, a recycle delay of 5 s, and WALTZ-16 ^1H decoupling [A. J. Shaka, J. Keeler, R. Freeman, *J. Magn. Reson.* **53**, 313 (1983)]. Data sets were zero filled once before Fourier transformation. Samples were 2.1 mM in GCN4-p1, 3.2 mM in GCN4-$p1_{15-27}$ (*24*), or 38 mM (by weight) in *N*-acetyl-glutamic acid α-methyl ester (AcGluOMe; Bachem Bioscience Inc., Philadelphia, PA) in 10 mM sodium phosphate, 150 mM NaCl containing 10% D_2O and referenced to 0 ppm with trimethylsilylpropionic acid.
25. Peptide concentrations were determined by tyrosine absorbance in 6 M guanidine hydrochloride assuming an extinction coefficient at 276 nm of 1500 M^{-1} cm^{-1} [H. Edelhoch, *Biochemistry* **6**, 1948 (1967)].
26. R. S. Hodges, J. Sodek, L. B. Smillie, L. Jurasek, *Cold*

Spring Harbor Symp. Quant. Biol. **37**, 299 (1972); D. A. D. Parry, *Biosci. Rep.* **2**, 1017 (1982); J. F. Conway and D. A. D. Parry, *Int. J. Biol. Macromol.* **12**, 328 (1990); A. Lupas, M. Van Dyke, J. Stock, *Science* **252**, 1162 (1991); B. Berger, D. B. Wilson, T. Tonchev, M. Milla, P. S. Kim, *Proc. Natl. Acad. Sci. U.S.A.*, in press.

27. pK_a values were determined at 25°C from a nonlinear least-squares fit of the change in chemical shift of the carboxylate ^{13}C-resonance with pH to the Henderson-Hasselbach equation [J. S. Cohen, R. I. Shrager, M. McNeel, A. N. Schechter, *Nature* **228**, 642 (1970)]. The pH was measured at room temperature before and after each NMR experiment and varied by less than 0.05 units. Because the largest source of uncertainty is systematic error in the measurement of pH, the experiments were performed in parallel (folded and unfolded in pairs), which reduces the error in the ΔpK_a values to less than the error in the measurement of the absolute value of any individual pK_a value. pK_a values measured in two independent sets of experiments agreed to within 0.05 units.

28. We are indebted to P. Harbury and B. Tidor for insightful discussions. We thank M. W. Burgess, S. Britt, and R. Rutkowski for peptide synthesis and mass spectrometry. Supported by grant GM44162 from the National Institutes of Health.

12 October, 1994; accepted 21 December, 1994

Nicotinic Receptor Binding Site Probed with Unnatural Amino Acid Incorporation in Intact Cells

Mark W. Nowak, Patrick C. Kearney, Jeffrey R. Sampson, Margaret E. Saks, Cesar G. Labarca, Scott K. Silverman, Wenge Zhong, Jon Thorson, John N. Abelson, Norman Davidson, Peter G. Schultz, Dennis A. Dougherty, Henry A. Lester*

The nonsense codon suppression method for unnatural amino acid incorporation has been applied to intact cells and combined with electrophysiological analysis to probe structure-function relations in the nicotinic acetylcholine receptor. Functional receptors were expressed in *Xenopus* oocytes when tyrosine and phenylalanine derivatives were incorporated at positions 93, 190, and 198 in the binding site of the α subunit. Subtle changes in the structure of an individual side chain produced readily detectable changes in the function of this large channel protein. At each position, distinct features of side chain structure dominated the dose-response relation, probably by governing the agonist-receptor binding.

In the study of membrane-bound receptor, channel, and transporter proteins, classical pharmacology has defined highly specific agonists and antagonists, and quantitative structure-activity studies have generated many hypotheses concerning ligand-receptor interactions. More recently, the combination of site-directed mutagenesis and heterologous expression has enabled functional studies of the consequences of structural modifications of the receptors. In the absence of atomic-scale structural data for membrane-bound receptors, these methods provide detailed information for the study of ligand-receptor interactions. First-generation mutagenesis methodologies used the normal translation machinery in such a way that a residue of interest could be changed to any of the other 19 natural amino acids.

Site-directed mutagenesis combined with nonsense suppressors [transfer RNAs (tRNAs) altered at the anticodon so that they insert an amino acid in response to an mRNA termination codon] have allowed the generation of several proteins with known amino acid changes from a single mRNA (*1*). Recently, second-generation mutagenesis methodologies have incorporated the nonsense suppression principle and extended the amino acid repertoire by providing a means for the site-specific incorporation of unnatural amino acids into proteins in cell-free systems (*2*, *3*). We report here the adaptation of this approach to a heterologous expression system in an intact cell. Combined with the high sensitivity and resolution of modern electrophysiological techniques, the incorporation of unnatural amino acids provides a general method for structure-function studies of receptors, channels, and transporters.

Figure 1A outlines the nonsense codon–tRNA suppressor method as adapted to intact eukaryotic cells. A *Xenopus* oocyte was coinjected with two mutated RNA species: (i) mRNA, synthesized in vitro from a mutated complementary DNA (cDNA) clone containing a stop codon, TAG, at the amino acid position of interest and (ii) a suppressor tRNA (*4*) containing the complementary anticodon sequence (CUA) and the desired unnatural amino acid synthetically acylated to the 3′ end (*5*, *6*). During translation by the oocyte's synthetic machinery, the unnatural amino acid was specifically incorporated at the appropriate position in the protein encoded by the mRNA.

We exploited this method to study a ligand-gated ion channel, the nicotinic acetylcholine (ACh) receptor (*7*). The muscle-type ACh receptor (AChR) contains five subunits with a stoichiometry of $\alpha_2\beta\gamma\delta$. An appropriate subject for this first investigation was the interaction between ligands

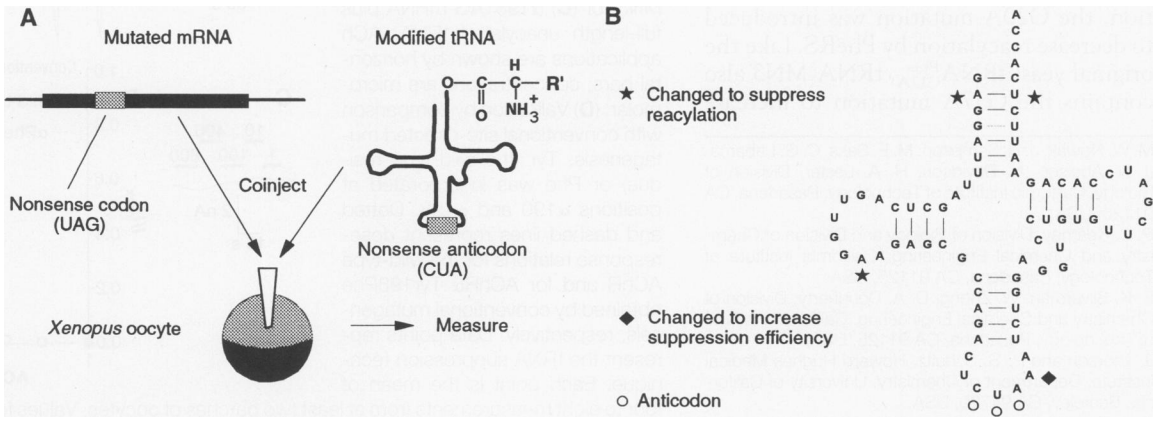

Fig. 1. (**A**) Strategy for unnatural amino acid incorporation into membrane proteins of intact *Xenopus* oocytes. The mRNA was generated from a cDNA clone in which the codon of interest had been mutated to a nonsense codon, TAG. The unnatural side chain is denoted as R′. (**B**) Structure of the nonsense suppressor tRNA-MN3, designed to maximize suppression efficiency and to minimize reacylation.